

NOAA Technical Memorandum NWS SR-208

**THE EASTER WEEKEND TORNADOES OF APRIL 3, 1999**

Mike Berry  
Weather Forecast Office  
Shreveport, Louisiana

Scientific Services Division  
Southern Region  
Fort Worth, Texas

February 2001

UNITED STATES  
DEPARTMENT OF COMMERCE  
Donald L. Evans, Secretary

National Oceanic and Atmospheric Administration  
Scott B. Gudes  
Under Secretary and Administrator (Acting)

National Weather Service  
John J. Kelly, Jr.  
Assistant Administrator  
for Weather Services



## 1. Introduction

The 1999 Easter weekend tornado outbreak across portions of extreme northeast Texas and northwest Louisiana was one of the most damaging and deadliest events in recent memory. The outbreak occurred in an area of the country where powerful tornadoes are not necessarily uncommon, but they are certainly infrequent. This paper examines certain atmospheric conditions on April 3, 1999, and dissects individual tornadic events using the WSR-88D radar located at the National Weather Service Office in Shreveport, Louisiana.

## 2. Pre-Storm Synoptic Environment

### a. Early Morning.

The upper air pattern on the morning of April 3 showed a strong potential for organized severe weather across the southern Plains and the lower Mississippi Valley. A deep, amplified trough was located across the southern Great Basin into the southern Rockies, with a mid-level ridge extending from the southeastern states into the upper Ohio Valley (Fig. 1). While a jet axis at 250 mb was located in the downstream side of the trough in the lee of the Rockies, a 60-70 kt jet streak was evident across east Texas and north Louisiana, with strong divergence across the same area (Fig. 2). The divergence was well correlated in the 700 mb Omega field across east Texas into north Louisiana, with a maximum across the southeast Texas coast (Fig. 3). A strong south-southwest 40-45 kt low-level jet was oriented along an 850mb Theta-e axis extending from south Texas into southern Missouri (Fig. 4). Theta-e moisture convergence was maximized across east Texas, southeast Oklahoma and southwest Arkansas as the 850 mb front approached north-central Texas.

The surface analysis at 1400 UTC (Fig. 5) showed a stationary front extending south from a low pressure center in northeast Kansas, to another area of low pressure across north Texas, and further south to the Big Bend area of southwest Texas. A north-south line of convection began to develop along and ahead of this surface boundary across north-central Texas as the boundary encountered abundant low-level moisture (dewpoints were in the upper 60s).

### b. Early Afternoon.

At 1800 UTC thunderstorms began developing in a northeast-southwest line, ahead of the initial line of convection, along a newly formed pre-frontal trough which extended from south-central Texas into northeast Oklahoma (Fig. 6). The 6-hr 250 mb forecast from the 1200 UTC Eta model run on April 3 continued to show a 60-70 kt jet streak from the Texas Big Bend into south Arkansas. This feature remained separated from the main jet axis which continued to deepen the upper trough over the Great Basin. At 500mb, embedded short waves rounded the base of the trough, which was likely too far west to immediately impact the afternoon weather pattern across the lower Mississippi Valley. Instead a small area of positive vorticity in the Big Bend area of Texas, quite innocent looking on the 1200 UTC April 3 Eta model initialization earlier that morning (Fig. 1), would provide sufficient dynamic forcing later in the day.

While the 6-hr Eta forecast at 500 b showed little more than a weak vorticity axis and minimal positive vorticity advection across east Texas and north Louisiana, the 0000 UTC April 4 Eta model

run initialized a considerably stronger vorticity axis across the lower Mississippi Valley compared to the previous Eta 12-hr forecast.

A low and mid-level cloud deck persisted through the early afternoon, while strong south winds at the surface increased warm air advection across the lower Mississippi Valley, ahead of the approaching pre-frontal trough. This warm air advection allowed afternoon temperatures to reach 80 F by 1800 UTC, with surface dewpoints approaching 70 F.

### **3. Sounding Analysis and Mesoscale Environment**

#### **a. Early Morning - Unmodified Environment.**

Analysis of the unmodified Shreveport sounding on the morning of April 3 indicated a highly unstable, highly sheared environment across the lower Mississippi Valley. The 1200 UTC sounding (Fig. 7) produced a minimum lifted index of -9 C, with a convective available potential energy (CAPE) value of 1739 J/Kg. A steep 850-500 mb lapse rate of 8 C/km was also present. The environmental wind field was very strong that morning as indicated by the Shreveport hodograph (Fig. 8) which showed 0-6 km shear in excess of 21 m/s. Mid-level winds in the 700-400 mb layer averaged 45 kt, complemented by ground-relative mean winds in the lowest 6 km of 39 kt from 217 deg. The NSHARP program (Hart et al., 1997) yielded a storm-relative helicity value in the 0-3 km layer of 388 m<sup>2</sup>/s<sup>2</sup>.

#### **b. Early Afternoon - Modified Environment.**

The early morning pre-storm environment based on the April 3 1200 UTC Shreveport sounding was modified to account for surface heating and low-level warm advection. With a surface temperature of 80F the modified sounding (Fig. 9) yielded a minimum LI of -13 C and CAPE increased to 2932 J/Kg. While the surface winds increased substantially from the south by early afternoon, the wind field in general stayed basically unchanged from the observed 1200 UTC observation, based on interpolation of the 1800 UTC wind field using the VAD wind profiler from the Shreveport WSR-88D. Warm advection during the morning hours helped to weaken the low-level capping inversion near 900 mb in the modified Shreveport sounding. Low-level forcing was maximized along the pre-frontal surface trough to the extent that when the shallow capping inversion was broken, thunderstorms began developing along the trough. This line of thunderstorms continued to grow and propagate northeast along the pre-frontal trough.

### **4. Doppler Radar Analysis**

By 2148 UTC the squall line oriented itself from north-central Arkansas southwest into extreme southeast Texas (Fig. 10). This line had a history of producing straight-line winds in excess of 60 mph across portions of northeast Texas, along with large hail up to one inch in diameter. East of the squall line, several thunderstorm clusters developed across extreme east-central Texas, northwest Louisiana, and southwest Arkansas. Some of these thunderstorms, initially multicellular in appearance, took on characteristics of supercell storms as they developed in the unstable, highly sheared environment.

a. The Shelby County Texas, De Soto Parish Louisiana Tornado.

Of the thunderstorm clusters which developed to the east of the squall line, this was the southernmost storm, thus this developing tornadic supercell had little if any competition in maximizing the amount of inflow into its updraft. At 2148 UTC the Shreveport WSR-88D showed the beginning of a hook echo in the 0.5 deg reflectivity data. The corresponding storm relative velocity (SRM) data at 0.5 deg showed greater than 45 kt of rotational velocity, with a gate-to-gate shear of greater than .051/s at an elevation of almost 2900 ft agl. Three minutes later, at 2151 UTC, a tornado touched down in northeast Shelby County, two miles southeast of Joaquin, Texas.

This supercell continued to exhibit hook-like characteristics on 0.5 deg reflectivity throughout its life span (Plate 1a). Likewise, the storm relative velocity continued to indicate a strong mesocyclone with high inbound and outbound gate-to-gate velocity signatures as the storm crossed the Sabine River and moved into De Soto Parish near Logansport, Louisiana (Plate 1b). Surveys after the event showed the tornado broadened rapidly to about 150 yd in diameter just before moving into De Soto Parish. The survey confirmed numerous homes suffered moderate to severe damage and the tornado uprooted or snapped several trees before lifting 2.6 mi northeast of Logansport at approximately 2159 UTC.

Figure 11 shows the rotational shear nomogram for tornadoes developed by Falk and Parker (1998). Based on the figure and the storm shear vs. range, the SRM signature for this tornado was classified "tornado likely."

b. The Caddo, Bossier Parish Tornado.

At 2152 UTC, one minute after the first tornado touched down southeast of Joaquin, Texas, a second tornado touched down 6.2 mi north of Shreveport. A strong hook echo became evident in the 0.5 deg reflectivity data at 2148 UTC. Because this signature was located so close to the local WSR-88D radar (approximately 6 mi), the corresponding storm relative velocity display had to be tilted to an elevation of 4.3 deg before rotation could be observed. At this elevation, the SRM rotational signature was rather broad in nature. The signature quickly tightened significantly and became an intense mesocyclone at 2158 UTC (at a beam elevation of 2.4 deg, or 3100 ft agl). SRM data at 2158 UTC (Plate 2b) shows this intense mesocyclone, which exhibited a rotational velocity of greater than 50 kt with a gate-to-gate shear in excess of .278/s and a diameter of 0.1 mi. The shear parameter is off the top of the scale in Fig. 11.

According to eyewitnesses, the tornado first touched down approximately 6.2 mi north of the Shreveport Regional Airport at 2152 UTC and moved northeast 6.7 mi before crossing the Red River and entering Bossier Parish. Ground surveys concluded that while the tornado was in Caddo Parish it exhibited F3 characteristics with a path width of 200 yd. This tornado would prove to be deadly as it moved into Bossier Parish at approximately 2201 UTC. The tornado continued to exhibit a hook-like signature in the 0.5 deg reflectivity data at 2208 UTC. The corresponding SRM image continued to indicate a strong gate-to-gate cyclonic signature in the wind field.

The storm produced catastrophic damage as it moved across the Hay Meadow Mobile Home Park and the Palmetto-Cypress Bayou areas of Bossier Parish before finally lifting at 2220 UTC. Aerial as well as ground surveys were conducted by state and federal officials who rated this tornado F4 in intensity (due to damage in Bossier Parish) with wind speeds in excess of 206 mph and a path width of 200 yd. Seven people lost their lives and 93 were injured. Hundreds of homes were damaged or destroyed throughout this tornado's 19 mi path across Caddo and Bossier Parishes. Damage estimates were in excess of \$20 million.

c. The Claiborne Parish Tornadoes.

As the northern half of the squall line accelerated eastward into northwest Louisiana, yet another mesocyclone developed ahead of this line in extreme southern Claiborne Parish. This storm separated itself from a cluster of multicellular storms farther west and became the lead storm, much like the earlier Shelby County/De Soto Parish storm. As a result, this storm was able to maximize the inflow into its updraft. A hook-like appendage can be seen wrapping around the storm's rear-flank downdraft (Plate 3a) just before the tornado was observed touching down at 2258 UTC. The corresponding storm relative velocity scan at 0.5 deg elevation or 3800 ft agl (Plate 3b) indicated a strong rotational signature with velocities in excess of 45 kt and gate-to-gate shear values in excess of .036/s. Applying the shear vs. range nomogram (Fig. 11) to this mesocyclone, the gate-to-gate shear falls under the "tornado likely" category.

This storm passed along the southeast side of Athens, Louisiana, before it lifted just to the southwest of Lake Claiborne at 2308 UTC. Eyewitnesses continued to see a funnel-like cloud protruding from the rear flank of the storm as it passed over the lake. The funnel remained off the ground for 8 mi before touching down a second time 8 mi southwest of Summerfield, Louisiana. While a hook was not apparent in reflectivity data during the second touchdown, a precipitation free inflow notch was seen along the southeast side of the storm. The tornado finally lifted 7.5 mi northeast of Summerfield at 2330 UTC, at which time there was a corresponding increase in diameter of inbound and outbound radar velocities in the 0.5 deg SRM scan.

Because there was an eight mile separation between touchdowns, the event was classified as two separate tornadoes, even though both were spawned by the same parent supercell as it moved north-northeast. Both tornadoes were later classified as F3 intensity from their damage patterns. Ground surveys after the event showed the path width increased at times to 500 yd. Nearly 25 homes were damaged or destroyed and numerous large trees were uprooted or snapped off.

## 5. Tornadogenesis

Much research has gone into the correlation of several environmental parameters with severe thunderstorm and tornado development. The parameters include environmental wind shear and storm relative helicity, with and without the combined effects of CAPE. A favorable wind profile in the storm inflow layer and the strength of this wind profile throughout a deep layer of the troposphere have been shown to correlate well with supercell development (Davies and Johns 1993). Figure 12 shows a distribution of the Davies and Johns data, comprising 240 tornado cases which suggest a shear value in the surface - 6 km layer in excess of 18 m/s is needed for tornado

development. A noticeable drop-off is noted in the number of tornado cases when the surface - 6 km shear exceeds 27 m/s. Davies and Johns suggest that while sufficient deep layer shear is needed for low-level mesocyclone development, too much shear can prove detrimental to sustaining a strong rotating updraft. A shear value of 21 m/s was calculated for the 0-6 km layer using NSHARP with the 1200 UTC April 3 Shreveport sounding, supporting the Davies and Johns conclusion.

In addition to deep layer shear, storm relative environmental helicity has long been used as a supercell parameter. Storm relative helicity is defined as the amount of shear a thunderstorm experiences relative to storm motion:

$$\text{Helicity} = \int \mathbf{w} \cdot (\mathbf{V} - \mathbf{V}_s) dz$$

where  $\mathbf{w} = \mathbf{k} \times d\mathbf{V}/dz$ ,  $\mathbf{V}$  being wind velocity and  $\mathbf{V}_s$  being storm velocity (Colquhoun and Riley 1996). It is suggested that when surface-3 km helicity values exceed  $150 \text{ m}^2\text{s}^2$ , then there is a higher potential for mesocyclone-induced tornadoes, dependent upon instability and forcing (Davies-Jones 1990). On April 3, the surface-3 km storm relative helicity based on the Shreveport sounding at 1200 UTC was  $388 \text{ m}^2\text{s}^2$ , more than double the value that Davies-Jones suggested.

While the strength and depth of environmental shear as well as storm relative helicity all pointed to the likelihood of long-lived mesocyclones and supercells on April 3, is there a parameter which could have predicted the possible strength of any tornadoes spawned that day? Hart and Korotky (1991) developed a method of correlating instability and helicity known as the Energy-Helicity Index (EHI), defined as:

$$\text{EHI} = \text{CAPE (H)}/160,000$$

where CAPE is the positive area on a sounding in association with the buoyancy of a lifted parcel between the level of free convection and the equilibrium level. Storm relative helicity between the surface and 3 km is represented by the term H. These advances were taken a step further by Davies (1993) who developed the following table as a guideline relating EHI to the severity of supercell oriented tornadoes.

less than 2.0	- significant mesocyclone-induced tornadoes unlikely
2.0 to 2.4	- mesocyclone-induced tornadoes possible but unlikely to be strong or long lived
2.5 to 2.9	- mesocyclone-induced tornadoes more likely
3.0 to 3.9	- strong tornadoes (F3) possible
4.0 +	- violent tornadoes (F4) possible

Based on the unmodified 1200 UTC Shreveport sounding on April 3, NSHARP computed an EHI value of 2.83, but when modified to account for the increased CAPE value that afternoon, the EHI increased to a dramatic 5.66, which falls well into Davies' category indicating the possibility of violent tornadoes.

## 6. Conclusions

A very unstable, highly sheared environment, combined with sufficient upward forcing and a low-level focusing mechanism, proved to be a volatile mix for tornado development on the afternoon of April 3, 1999. While the dynamic parameters that morning indicated the possibility of supercell-generated tornadoes during the afternoon, the magnitude of the tornadoes which formed could not have been known, or could they?

With the deployment and commissioning of AWIPS as well as computer programs such as NSHARP, forecasters have now been given a new array of tools to analyze and forecast a variety of different synoptic and mesoscale parameters. While the basic model data forecasters use and the methods in which sounding data are gathered have changed very little over the years, what has changed is the way model and observed data can now be dissected, and therefore interpreted, to forecast severe weather outbreaks.

Another advantage AWIPS provides in the modern National Weather Service office is its capability to display WSR-88D radar data. This not only gives meteorologists the ability to use multiple consoles in a storm situation, but in the case of the April 3 outbreak it provides for quicker action when tornadoes occur nearly simultaneously. Without this, while dissecting low-level reflectivity and velocity products for the tornado which touched down in Shelby County in Texas, a timely warning for the Caddo and Bossier Parish tornado could have easily been missed due to its rotational signal being apparent only at higher elevations. While further advances and study are needed in the areas of tornadogenesis and the meteorological conditions which are associated, this new technology will allow the meteorologist to apply and test theories which have already been established so that future tornadic events can be better understood and predicted.

## 7. Acknowledgments

This author appreciates the review and recommendations of WFO Shreveport MIC Lee Harrison, SOO Ken Falk and DAPM Marion Kuykendall, along with others on the operational staff. Special thanks go to Matthew Foster for his expertise in NAWIPS and his assistance in preparing figures for this study.

## 8. References

- Colquhoun, J.H., and Riley, P.A., 1996: Relationships Between Tornado Intensity and Various Wind and Thermodynamic Variables. *Wea. Forecasting*, **11**, 360-371.
- Davies, J., M., 1993: *Hourly Helicity, Instability and EHI in Forecasting Supercell Tornadoes*. Preprints - 17<sup>th</sup> Conf. on Severe Local Storms, St. Louis, Missouri, American Meteorological Society, 107-111.
- Davies - Jones, R., and Burgess, D. 1990: *Test of Helicity as a Tornado Forecast Parameter*. Preprints - 16<sup>th</sup> Conf. of Severe Local Storms, Kanaskis Park, Alta., Canada, American Meteorological Society, 588-592.

- Davies, J.M., and Johns, R.H., 1993: Some Wind and Instability Parameters Associated with Strong and Violent Tornadoes 1. Wind shear and Helicity. *The Tornado: Its Structure, Dynamics, Prediction and Hazards*, American Geophysical Union. 573-582.
- Falk, K.W., and Parker, William, 1998: *Rotational Shear Nomograms for Tornadoes*. Preprints - 19<sup>th</sup> Conf. on Severe Local Storms, Minneapolis, Minnesota, September, 1998, American Meteorological Society, 733-735.
- Hart, J.A., and Korotky, W.D., 1991: *The Sharp Workstation User's Manual*. NOAA/NWS, National Weather Service Office, Charleston, WV.
- Hart, J.A., Lindsay, Robert, and Whistler, Jim, 1997: *Sharp -v3.01(beta) Advanced Interactive Sounding Analysis for NAWIPS*. NOAA/NWS, Storm Prediction Center, Aviation Weather Center.

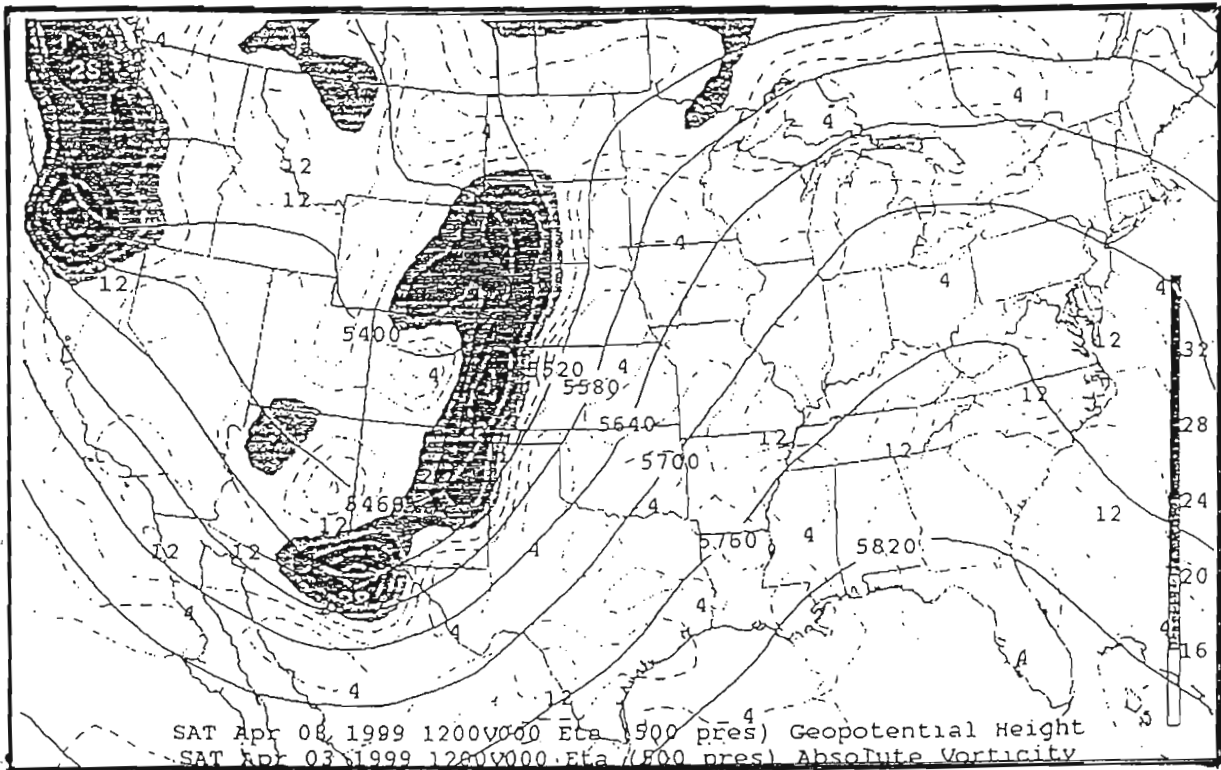


Fig. 1. Eta 500 mb height/vorticity at 1200 UTC April 3, 1999.

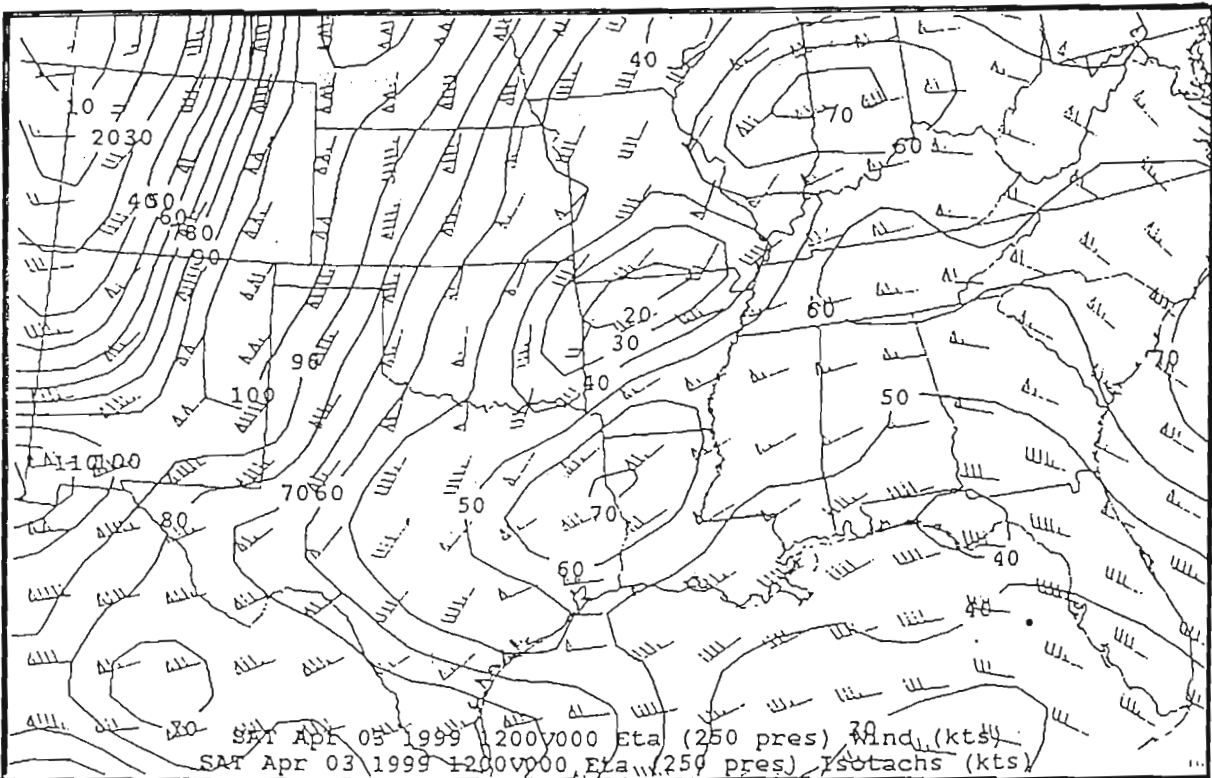


Fig. 2. Same as Fig. 1 except 250 mb wind and isotach analysis.

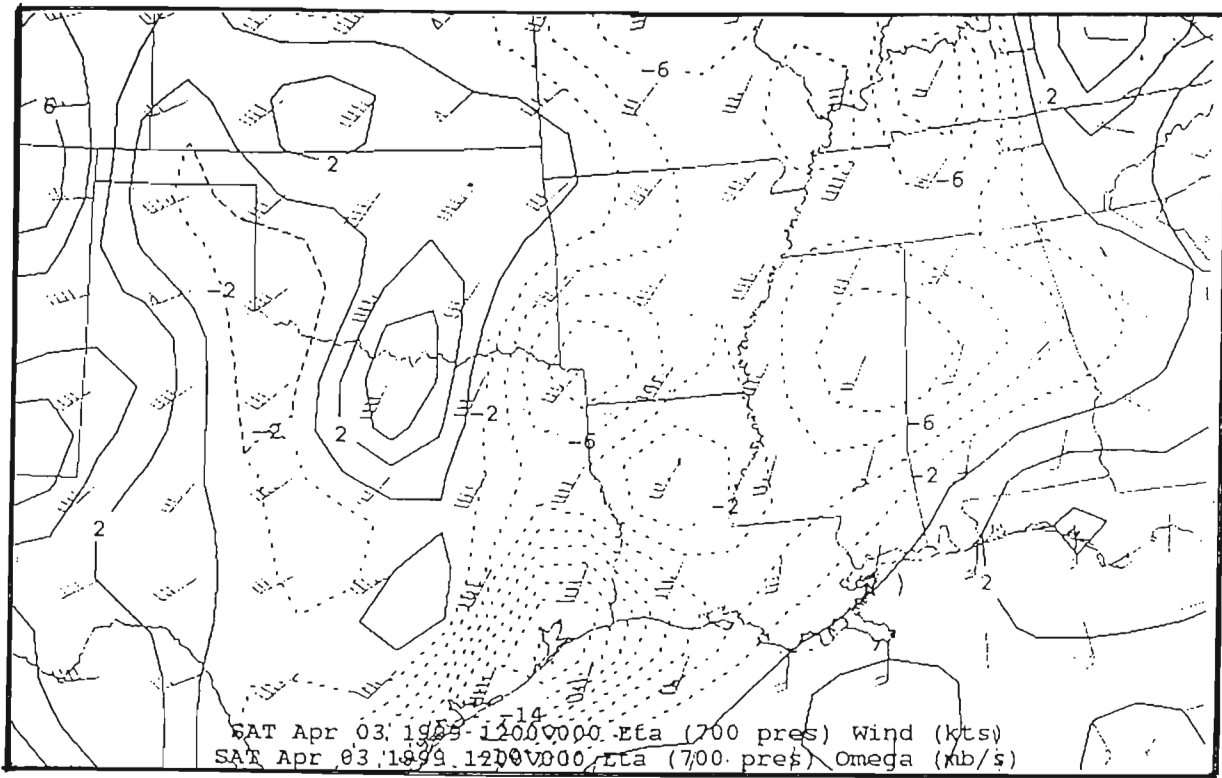


Fig. 3. Same as Fig. 1 except 700 mb wind and omega analysis.

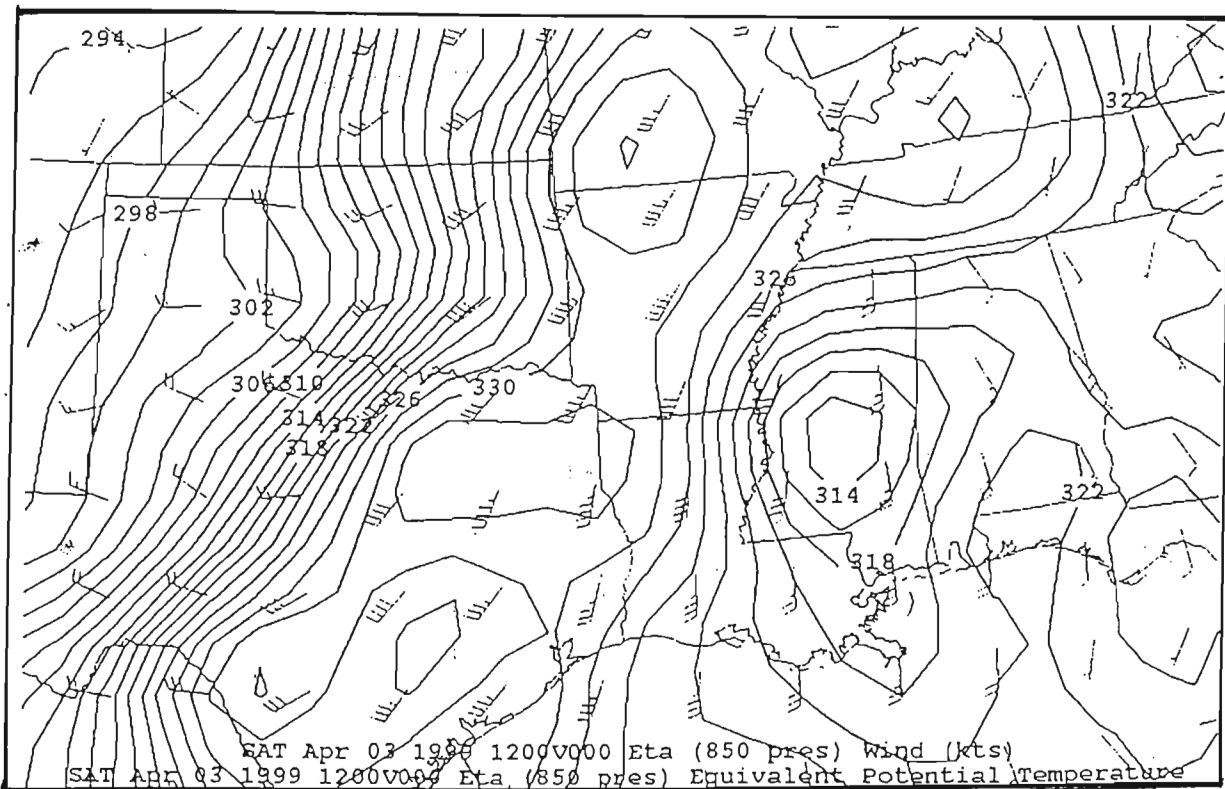


Fig. 4. Same as Fig. 1 except 850 mb wind and equivalent potential temperature analysis.

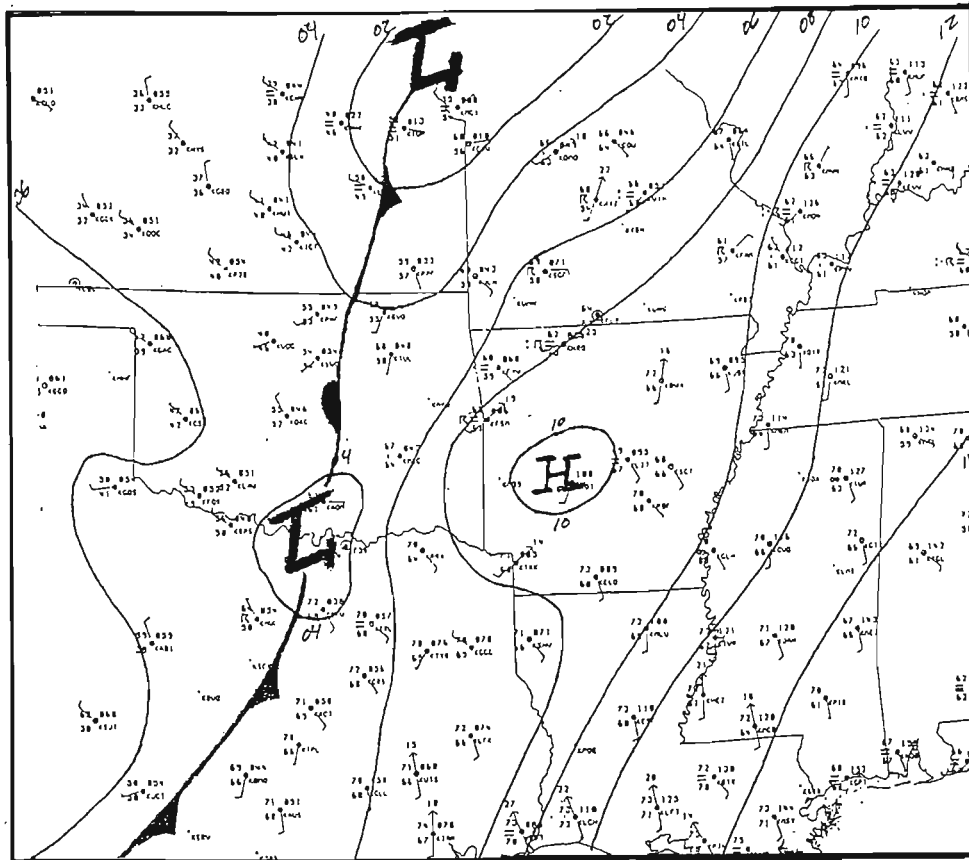


Fig. 5 Surface analysis at 1400 UTC April 3, 1999.

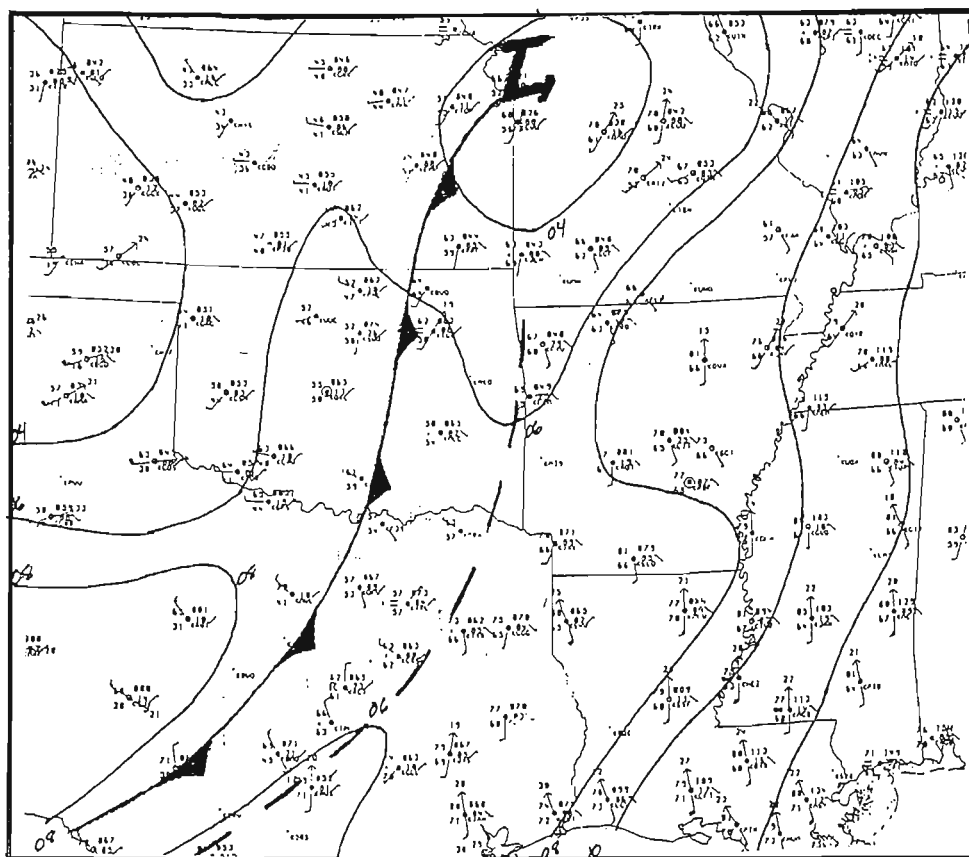


Fig. 6. Surface analysis at 1800 UTC April 3, 1999.

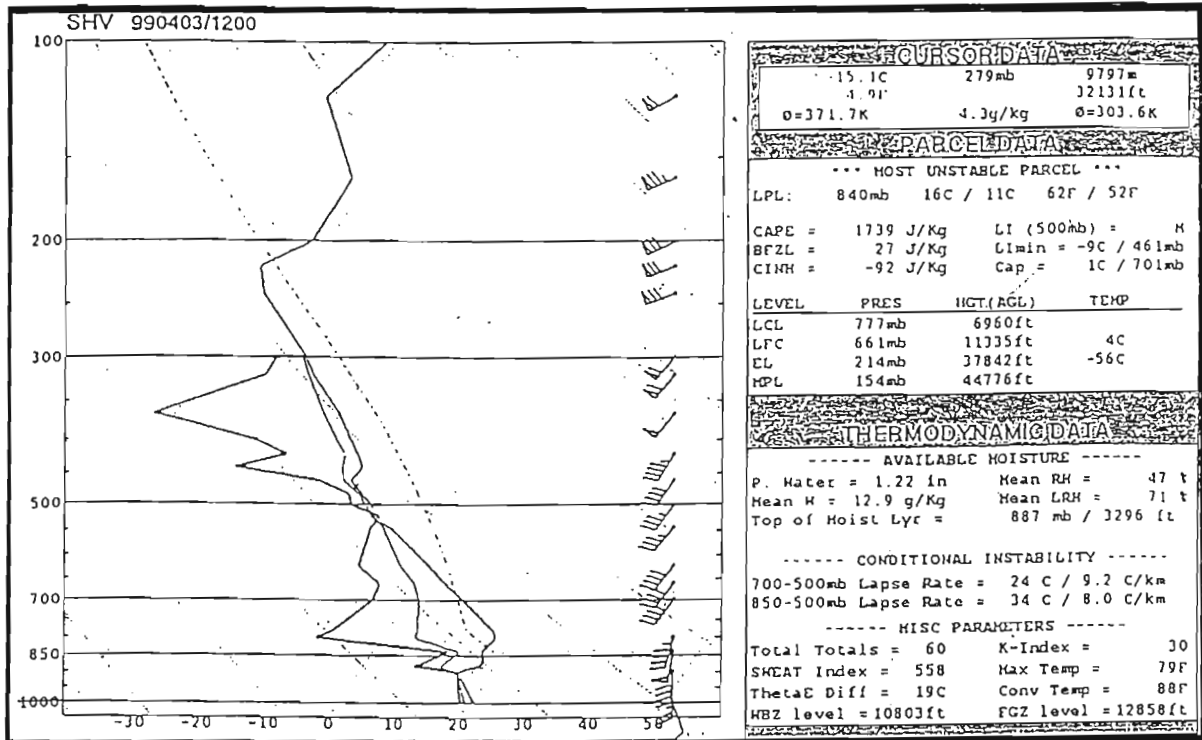


Fig 7. Sounding analysis from WFO Shreveport, 1200 UTC April 3, 1999.

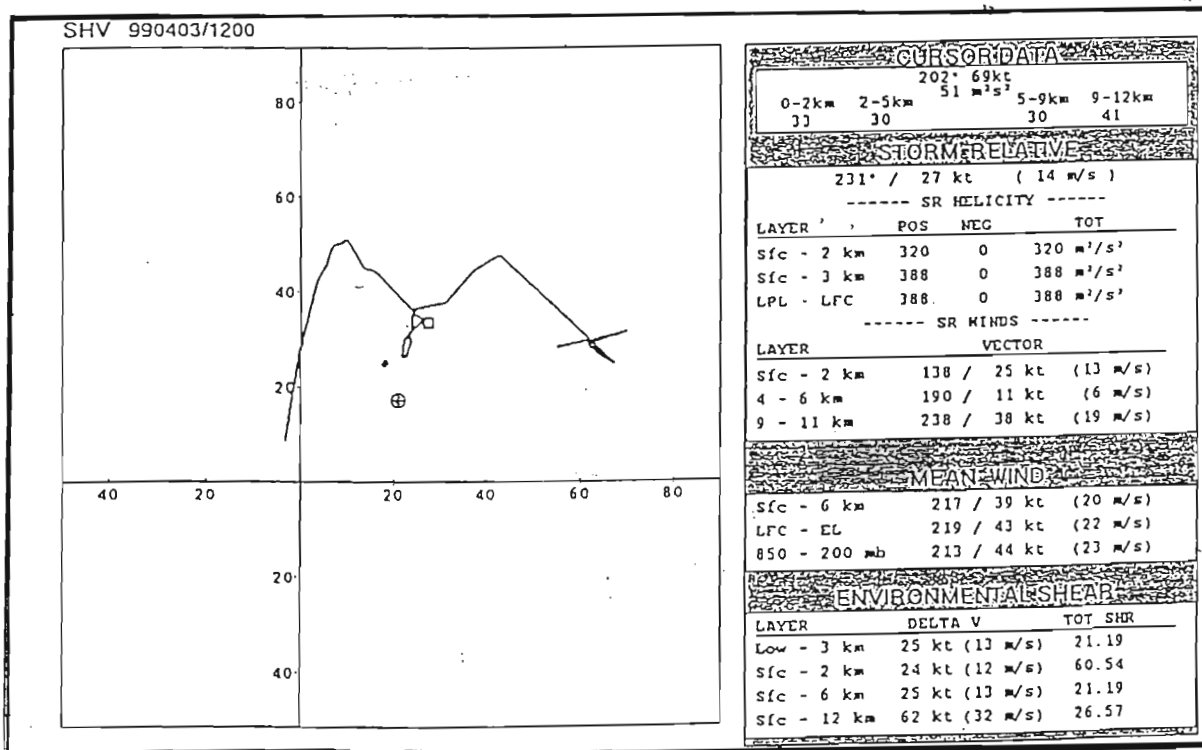


Fig 8. Observed wind hodograph from WFO Shreveport, 1200 UTC April 3, 1999.

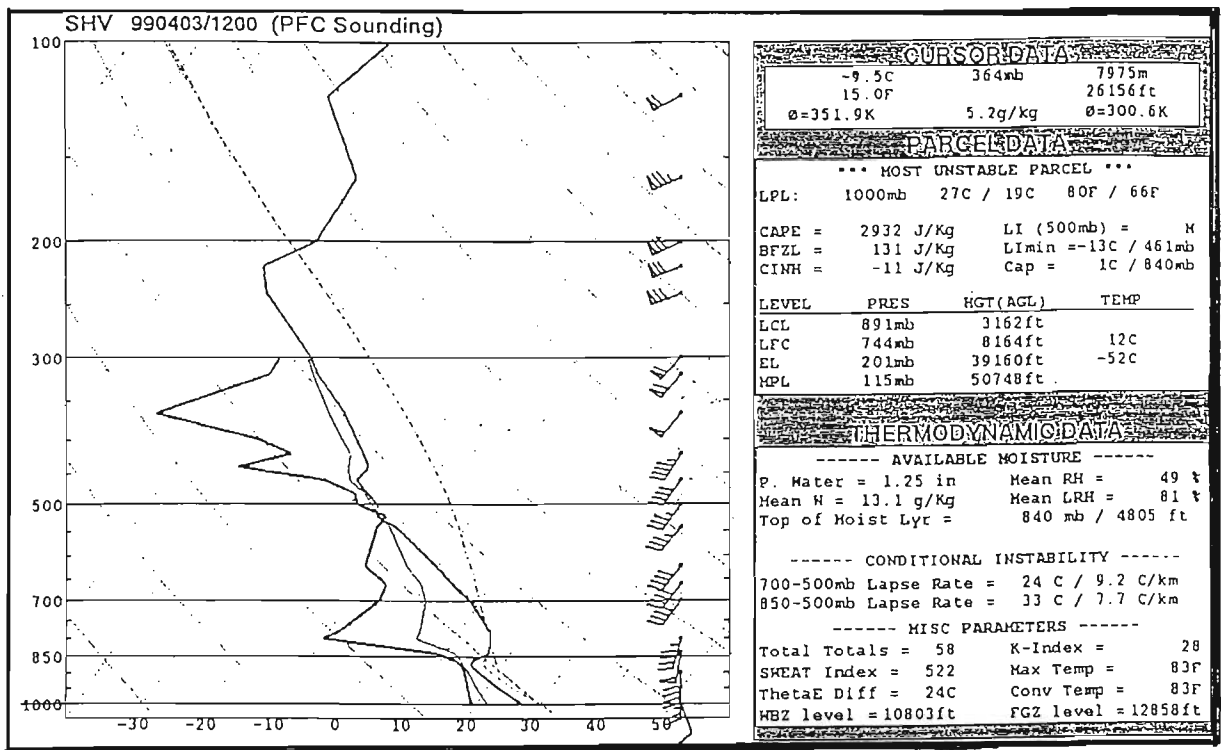


Fig. 9. Modified Shreveport sounding from April 3, 1999.

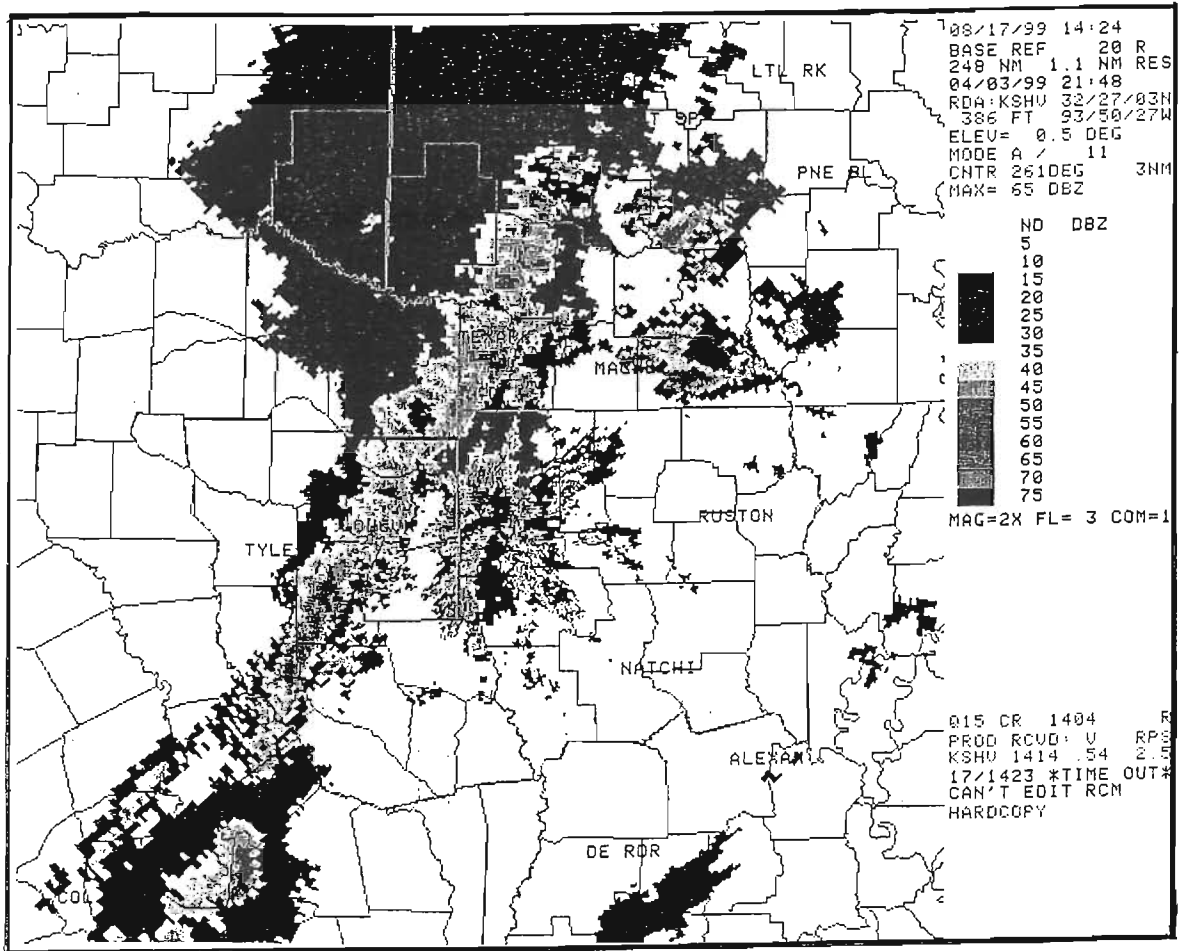


Fig. 10. WFO Shreveport WSR-88D 0.5 deg reflectivity, 2148 UTC April 3, 1999.

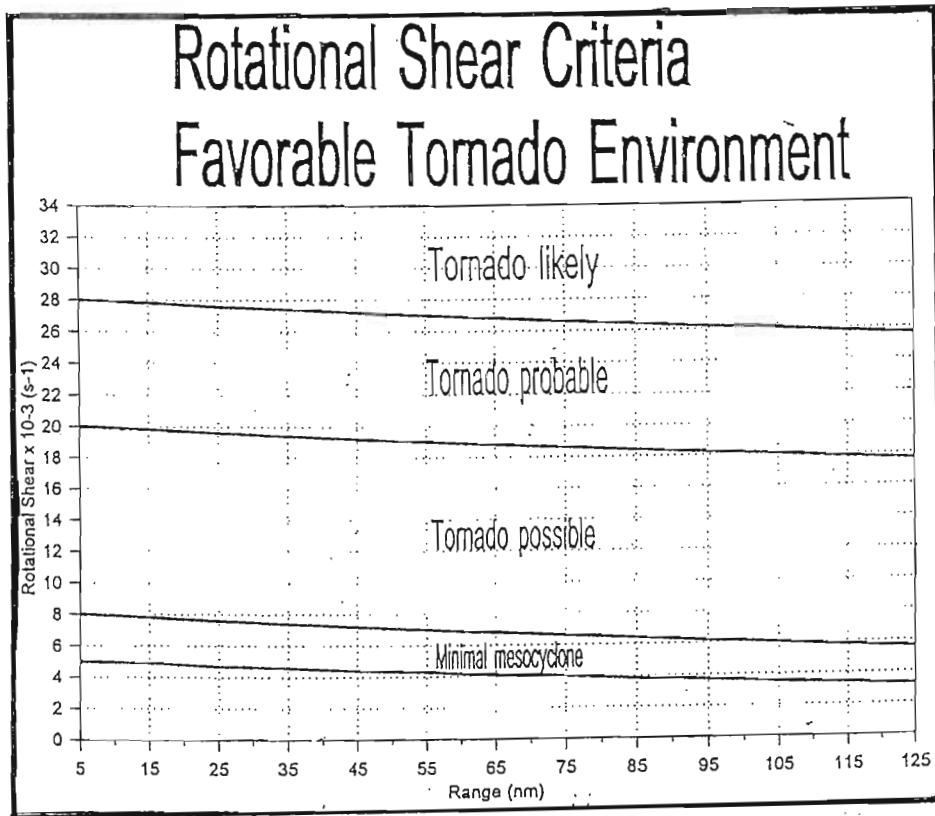


Fig. 11. Rotational shear vs. range nomogram (from Falk and Parker, 1998).

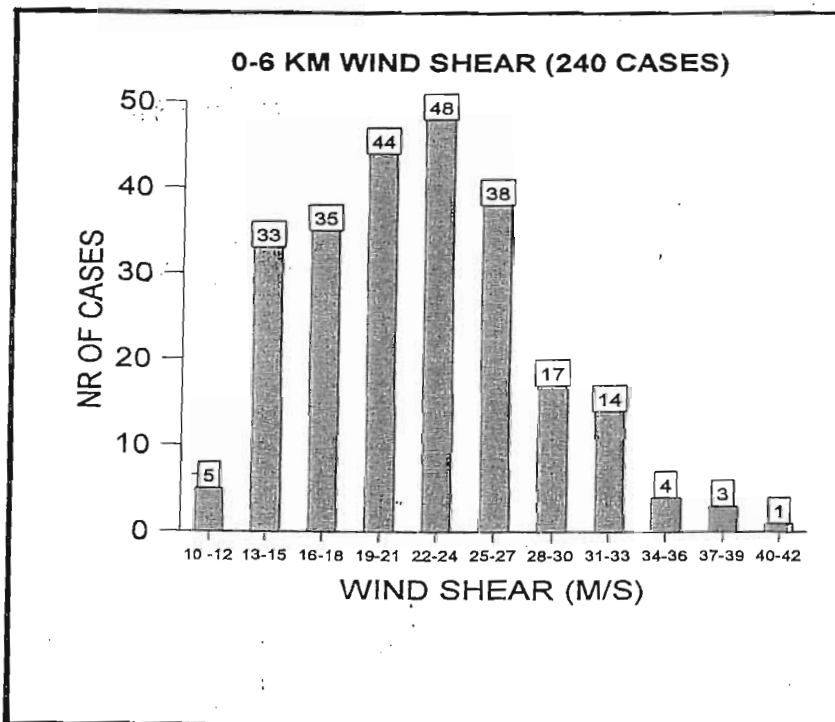
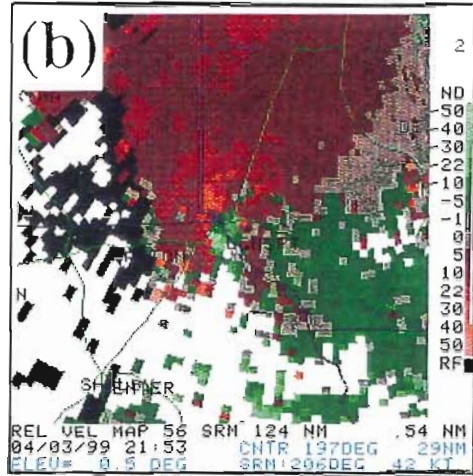
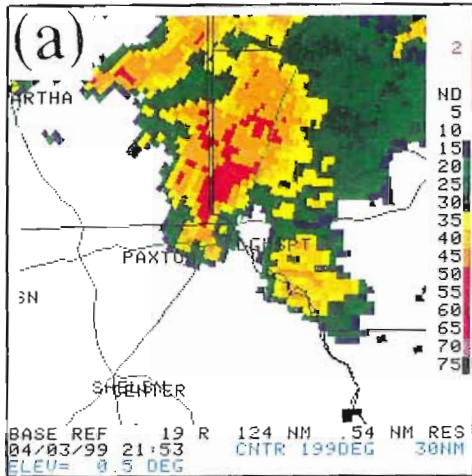
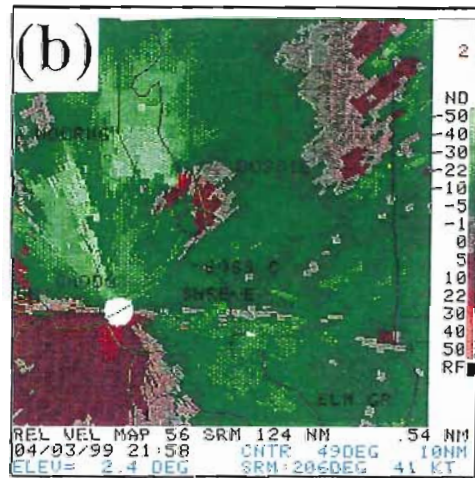
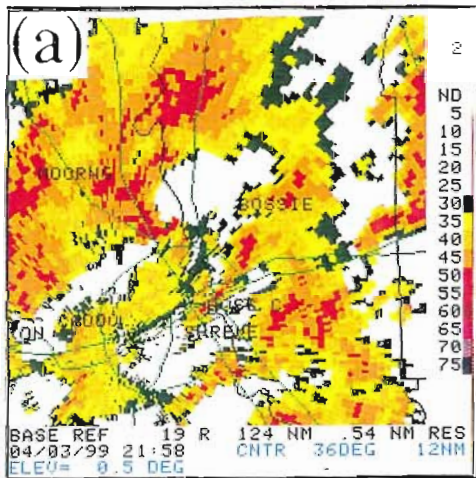


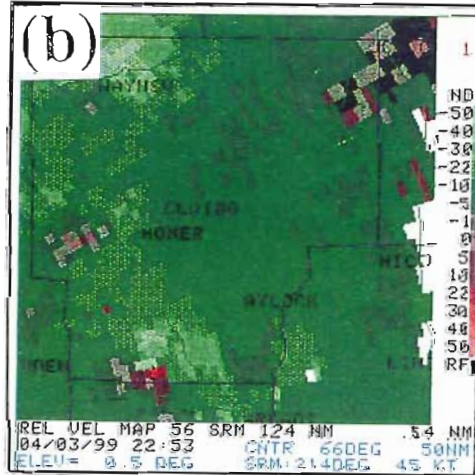
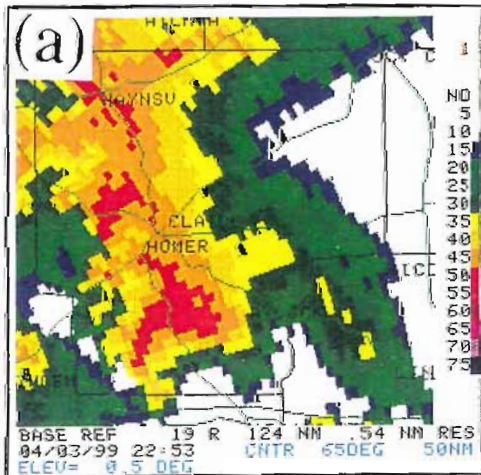
Fig. 12. Distribution of cases from JDL data set, grouped to shear magnitude. See text for details.



Color Plate 1. KSHV 0.5 deg. Reflectivity and Storm Relative Velocity of Shelby County, De Soto Parish tornado on 04/03/99, 2153 GMT.



Color Plate 2. KSHV 0.5 deg. Reflectivity, 2.4 deg. Storm Relative Velocity of Caddo, Bossier Parish tornado on 04/03/99, 2158 GMT.



Color Plate 3. KSHV 0.5 deg. Reflectivity and Storm Relative Velocity of Claiborne Parish tornado on 04/03/99, 2253 GMT.